Trust & Quality

Inspecta

INSPECTA

TECHNICAL REPORT

SKB

Statistical data analysis of cast iron properties for PWR-inserts from tension, compression and fracture toughness testing

Report No.: 50017490-1

Revision No.: 2

INSPECTA TECHNOLOGY AB

BOX 30100 104 25 STOCKHOLM SWEDEN TEL (+46) 8 5011 3000 FAX (+46) 8 5011 3001 www.inspecta.com

Date	Our project No.
2013-12-22	50017490
Approved by: Annika Haglund	Organizational unit: Inspecta Technology AB
Customer: SKB	Customer reference: Mikael Jonsson

Summary

SKB has commissioned Inspecta Technology AB to perform a statistical data analysis of material properties for cast iron PWR-inserts IP23, IP24 and IP25. The test data from tension, compression and fracture toughness tests were analysed.

The main purpose of the performed statistical analysis was to obtain the estimates of material properties with a given confidence (90% confidence was used in the analyses). Approximate confidence intervals using the so-called Student's *t*-distribution and the χ^2-distribution were calculated for all measured properties of the cast iron material. These confidence intervals provide a range where the true value of a material property is expected to lie.

Additionally, the performed analysis was aimed to investigate; 1) the variation of material properties between different PWR-inserts and 2) the variation of properties depending on the position where the specimens were taken.

The short conclusions of this investigation are following;

- Variation of properties between different PWR-inserts could be best studied from the tensile test results as substantial amount of data was collected. It could be observed that the yield strength and ultimate strength were lower for the material from the PWR-insert IP24. The tensile properties from the IP23 and IP25 inserts were higher and comparable with each other.
- Certain variation of tensile properties along the insert height was observed from the test data. For all tested PWR-inserts the mean values of the yield strength and the ultimate strength at the top (T) position were higher than for the middle and the bottom positions.
- Large variation of tensile properties depending on the cross-sectional position of a specimen was only observed for the cast iron material IP23T. For other PWR-inserts and tested cross-sections the variation of tensile properties was insignificant.
- Compression properties were only measured for the IP23M material. The variation of the properties depending on the cross-sectional position of the specimens was insignificant.
- Fracture toughness values appear to be somewhat lower for the specimens from the top (T) position in comparison with the middle and the bottom positions. The mean values of fracture toughness at initiation and at 2 mm stable crack growth were almost twice higher from the tests in air compared with the tests in water.
- Because of the process deviation for insert IP23, it is recommended to use fracture toughness data without IP23T when performing a damage tolerance analysis.

Report title	Subject Group / Index terms
Statistical data analysis of cast iron properties for PWR-inserts from tension, compression and fracture toughness testing	Subject Group: Index terms: PWR, Canister inserts, Material properties, Tension, Compression, Fracture toughness
Work carried out by: Andrey Shipsha	Distribution: ☒ No distribution without permission from the customer or Inspecta Technology AB. ☐ Limited internal distribution in Inspecta Technology AB. ☐ Unrestricted distribution.
Work verified by: Peter Dillström	

Table of content *Page*

1 INTRODUCTION

SKB has commissioned Inspecta Technology AB to perform a statistical data analysis of material properties for cast iron PWR-inserts IP23, IP24 and IP25. The test data from tension, compression and fracture toughness tests is analysed.

2 SHORT BASIS FOR STATISTICAL ANALYSIS

This section presents the main equations used for statistical analysis of the test data for cast iron PWR-inserts.

The sample mean value m is calculated as:

$$m = \frac{1}{n}\sum_{i=1}^{n} x_i \tag{2.1}$$

where n = number of samples.

The unbiased sample standard deviation s (the square root of the unbiased sample variance) is given as:

$$s = \sqrt{\frac{1}{n-1}\sum_{i=1}^{n}(x_i - m)^2} \tag{2.2}$$

For a given sample, these parameters are single-valued estimates of the mean and standard deviation of the analysed material property. The single-valued estimates represent a best estimate of the population values. In a damage tolerance analysis we want to use an estimate with a given confidence (i.e. 90%). Thus we are interested in the accuracy of these sample estimates. Confidence intervals represent a means of providing a range of values in which the true value can be expected to lie. In this investigation we will use approximate confidence intervals, using properties of the so-called Student's t-distribution and the χ^2-distribution [1].

Confidence interval for the population mean μ, when the population standard deviation σ is unknown, has the following form:

$$m - t_{\alpha/2,n-1}\left(\frac{s}{\sqrt{n}}\right) \le \mu \le m + t_{\alpha/2,n-1}\left(\frac{s}{\sqrt{n}}\right), \tag{2.3}$$

where $t_{\alpha/2,n-1}$ is the Student's t-distribution (using a two-sided interval) with a level of significance α and with $n-1$ degrees of freedom.

The confidence intervals given above now provide an interval in which we are $100(1-\alpha)$ per cent confident that the population values lies within that given interval.

3 DATA ANALYSIS

3.1 Tensile tests

3.1.1 Test specimen positions

Tensile tests of cast iron material were performed for three PWR-inserts IP23, IP24 and IP25 [2-11, 19]. The PWR-inserts were sectioned into discs at different levels along the vertical axis; at the top (T), in the middle (M), at the bottom (B) and in the homogeneous bottom (HB) as schematically shown in Fig 3.1 (a). From each cross-sectional disc eight (8) specimens were taken at the positions as numbered in Figure 3.1 (b).

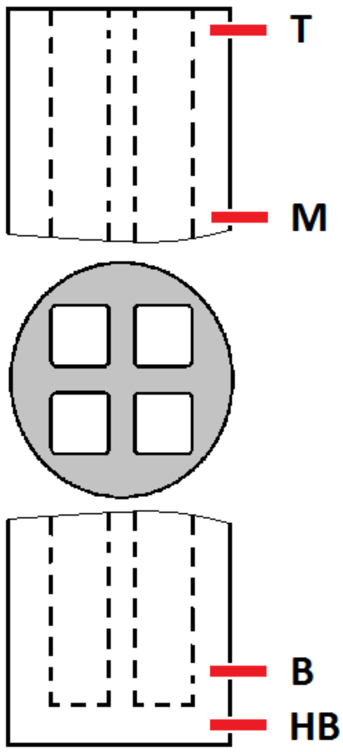

(a)

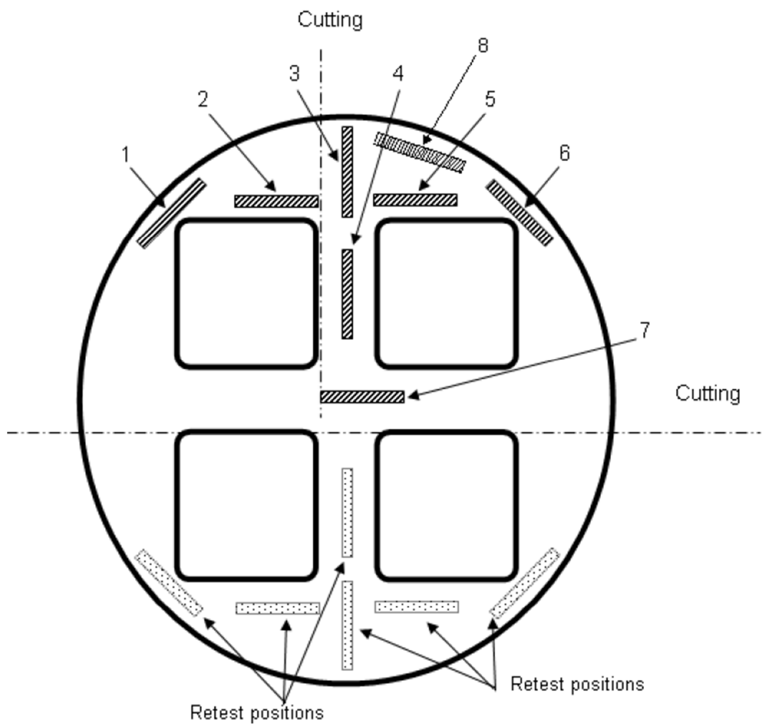

(b)

Figure 3.1: A schematic of the PWR-insert explaining the positions for specimen extraction; (a) a lateral view of the PWR-insert with marked levels along the vertical axis, (b) a cross-sectional view of the PWR-insert with marked positions for cutting the specimens for tensile testing.

3.1.2 Test data analysis

Yield strength, ultimate strength and elongation at failure of cast iron material were measured in tensile tests. These properties were statistically evaluated using Eqs. (2.1-2.3) in order to obtain a mean estimate along with the confidence intervals (90% confidence). The results per PWR insert are summarized in Tables 3.1-3.3. The engineering stress and strain definitions are used for the presented values. It should be observed that the results for the homogeneous bottom (HB) are only available for the IP23-insert. Specimen ID number in Tables 3.1-3.3 corresponds to the marked positions in Fig. 3.1 (b) except for the test set IP25M-2 containing only 5 specimens. For the set IP25M-2 the specimen 3 corresponds to the position 3, see Fig. 3.1 (b), but the specimens 1, 2 and 4, 5 are cut out close to the specimen 3, on the left and on the right hand side, respectively. The orientation for all five specimens in the IP25M-2 set is identical as shown for the position 3 (Fig. 3.1 (b)).

Table 3.1: IP23-insert. Tensile properties [2-5] and estimates of the population mean (90% confidence).

	Specimen	Yield strength $R_{p0.2}$ (MPa)	Ultimate strength R_m (MPa)	Elongation at failure $A5$ (%)
IP23T	1	290	435	15.4
	2	294	441	11.9
	3	274	411	19.3
	4	290	437	12.4
	5	300	450	10.6
	6	289	437	15.7
	7	275	413	19.7
	8	290	422	6.6
	Sample mean m	287.8	430.8	14.0
	Sample standard deviation s	8.9	13.9	4.5
	Population mean μ	$281.8 \leq \mu \leq 293.7$	$421.4 \leq \mu \leq 440.1$	$11.0 \leq \mu \leq 16.9$
IP23M	1	267	398	21.9
	2	266	395	15.8
	3	266	396	15.7
	4	279	380	4.9
	5	268	397	17.8
	6	269	399	22.4
	7	268	391	10.2
	8	268	395	19.9
	Sample mean m	268.9	393.9	16.1
	Sample standard deviation s	4.2	6.1	6.0
	Population mean μ	$266.0 \leq \mu \leq 271.7$	$389.8 \leq \mu \leq 398.0$	$12.1 \leq \mu \leq 20.1$
IP23B	1	266	400	21.9
	2	271	408	18.2
	3	265	401	20.5
	4	272	404	13.6
	5	272	409	19.8
	6	268	402	22.9
	7	270	403	21.4
	8	269	403	18.2
	Sample mean m	269.1	403.8	19.6
	Sample standard deviation s	2.6	3.2	2.9
	Population mean μ	$267.4 \leq \mu \leq 270.9$	$401.6 \leq \mu \leq 405.9$	$17.6 \leq \mu \leq 21.5$
IP23HB	1	271	408	21.1
	2	266	400	19.8
	3	270	402	19.8
	4	268	403	21.5
	5	269	401	20.8
	6	270	406	21.5
	Sample mean m	269.0	403.3	20.8
	Sample standard deviation s	1.8	3.1	0.8
	Population mean μ	$267.5 \leq \mu \leq 270.5$	$400.8 \leq \mu \leq 405.9$	$20.1 \leq \mu \leq 21.4$

Table 3.2: IP24-insert. Tensile properties [6-8] and estimates of the population mean (90% confidence).

	Specimen	Yield strength $R_{p0.2}$ (MPa)	Ultimate strength R_m (MPa)	Elongation at failure $A5$ (%)
IP24T	1	257	388	22
	2	259	388	18.7
	3	260	392	14.6
	4	267	401	12.3
	5	260	392	16.6
	6	260	389	22.2
	7	260	394	17.7
	8	258	389	18.1
	Sample mean m	260.1	391.6	17.8
	Sample standard deviation s	3.0	4.4	3.4
	Population mean μ	$258.1 \leq \mu \leq 262.1$	$388.7 \leq \mu \leq 394.6$	$15.5 \leq \mu \leq 20.0$
IP24M	1	259	387	19.7
	2	259	387	19.7
	3	256	388	18.6
	4	261	391	14.3
	5	256	381	11.8
	6	262	389	21.1
	7	260	386	11.9
	8	261	387	18.8
	Sample mean m	259.3	387.0	17.0
	Sample standard deviation s	2.3	2.9	3.7
	Population mean μ	$257.7 \leq \mu \leq 260.8$	$385.1 \leq \mu \leq 388.9$	$14.5 \leq \mu \leq 19.5$
IP24B	1	254	389	20.9
	2	254	388	20.3
	3	255	390	20.3
	4	261	396	14.9
	5	256	392	19
	6	256	392	22.5
	7	261	392	20.8
	8	258	392	20.5
	Sample mean m	256.9	391.4	19.9
	Sample standard deviation s	2.9	2.4	2.2
	Population mean μ	$255.0 \leq \mu \leq 258.8$	$389.7 \leq \mu \leq 393.0$	$18.4 \leq \mu \leq 21.4$

Table 3.3: IP25-insert. Tensile properties [9-11, 19] and estimates of the population mean (90% confidence).

	Specimen	Yield strength $R_{p0.2}$ (MPa)	Ultimate strength R_m (MPa)	Elongation at failure $A5$ (%)
IP25T	1	275	407	15
	2	280	415	14.1
	3	276	408	10.5
	4	283	422	12.4
	5	280	413	12.5
	6	276	406	16
	7	275	414	13.9
	8	276	403	12.4
	Sample mean m	277.6	411.0	13.4
	Sample standard deviation s	3.0	6.1	1.7
	Population mean μ	$275.6 \leq \mu \leq 279.6$	$406.9 \leq \mu \leq 415.1$	$12.2 \leq \mu \leq 14.5$
IP25M-1	1	271	396	13.6
	2	270	395	12.2
	3	270	399	16.8
	4	275	395	9.4
	5	270	397	13.7
	6	270	397	16.7
	7	263	377	8.0
	8	271	396	16.2
	Sample mean m	270.0	394.0	13.3
	Sample standard deviation s	3.3	7.0	3.3
	Population mean μ	$267.8 \leq \mu \leq 272.2$	$389.3 \leq \mu \leq 398.7$	$11.1 \leq \mu \leq 15.5$
IP25M-2	1	269	390	10.9
	2	271	391	10.4
	3	271	392	11.3
	4	272	392	11
	5	271	390	10.5
	Sample mean m	270.8	391.0	10.8
	Sample standard deviation s	1.1	1.0	0.4
	Population mean μ	$269.8 \leq \mu \leq 271.8$	$390.0 \leq \mu \leq 392.0$	$10.5 \leq \mu \leq 11.2$
IP25B	1	270	403	20.7
	2	272	403	17.6
	3	267	401	20
	4	273	407	19.8
	5	273	405	17.4
	6	270	402	16.7
	7	268	402	19.1
	8	271	403	19.3
	Sample mean m	270.5	403.3	18.8
	Sample standard deviation s	2.2	1.9	1.4
	Population mean μ	$269.0 \leq \mu \leq 272.0$	$402.0 \leq \mu \leq 404.5$	$17.9 \leq \mu \leq 19.8$

Statistical analysis of all tensile data from the three PWR-inserts is presented in Table 3.4 (using the engineering stress-strain definition) and in Table 3.5 (using the true stress-strain definition).

Table 3.4: Evaluation of all tensile data (engineering stress-strain definition). Tensile properties and estimates of the population mean (90% confidence).

All tensile data (83 specimens)	**Yield strength** $R_{p0.2}$ **(MPa)**	**Ultimate strength** R_m **(MPa)**	**Elongation at failure** $A5$ **(%)**
Sample mean m	269.0	400.3	16.6
Sample standard deviation s	9.3	13.5	4.3
Population mean μ	$267.3 \leq \mu \leq 270.7$	$397.9 \leq \mu \leq 402.8$	$15.8 \leq \mu \leq 17.4$

Table 3.5: Evaluation of all tensile data (true stress-strain definition). Tensile properties and estimates of the population mean (90% confidence).

All tensile data (83 specimens)	**Yield strength (MPa)**	**Ultimate strength (MPa)**	**Elongation at failure (%)**
Sample mean m	269.8	460.5	14.5
Sample standard deviation s	9.4	18.9	3.3
Population mean μ	$268.1 \leq \mu \leq 271.6$	$457.1 \leq \mu \leq 464.0$	$13.9 \leq \mu \leq 15.2$

3.1.3 Discussion of results

3.1.3.1 Variation of properties between inserts

Variation of tensile properties (engineering stresses) between three tested inserts is shown in Figure 3.2. The mean values of yield and ultimate strength are observed to be lowest for the cast iron material from the IP24-insert. The properties between the IP23 and IP25 inserts are found very similar.

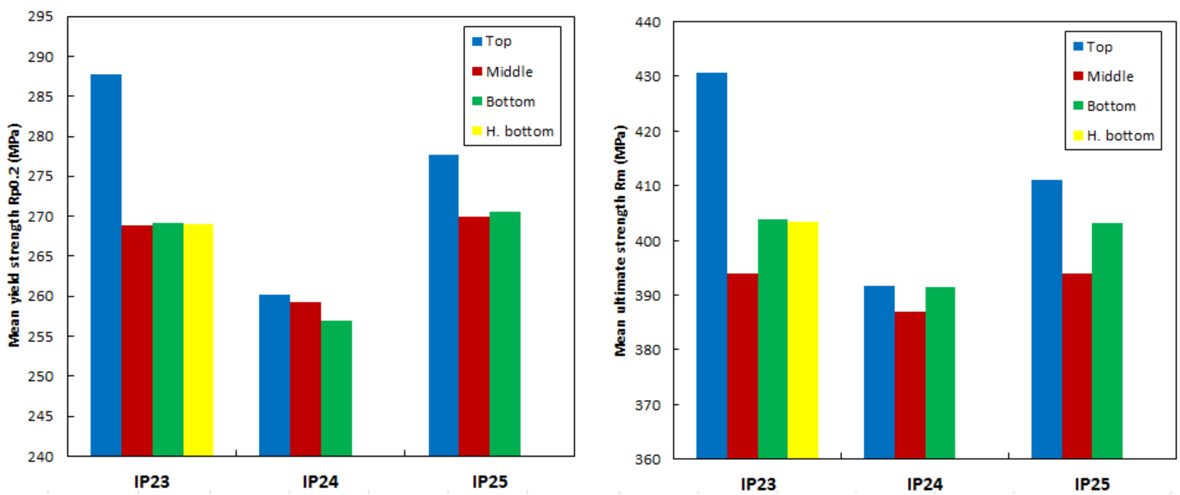

Figure 3.2: Variation of mean values of yield strength and ultimate strength between the PWR-inserts and effect of the position along the vertical axis of the insert. Engineering stress values are presented.

3.1.3.2 Variation of properties along the insert height

Variation of tensile properties (engineering stresses) along the insert height is shown Figure 3.2. For all tested PWR-inserts it was observed that the mean values of the yield strength and the ultimate strength at the top (T) position (Figure 3.1(a)) are substantially higher than for the middle and the bottom positions. Almost no variation in the yield strength was observed for the middle and the bottom positions for all inserts. The tensile properties in the homogeneous bottom (IP23 insert) are very similar to the bottom position.

The ultimate strength in the middle position was found lower in comparison to the top and the bottom positions for all PWR-inserts, see Figure 3.2 (right).

3.1.3.3 Variation of properties in the cross-section

The cross-sectional positions for cutting the specimens are shown in Figure 3.1(b). It can be noticed that the positions 1 and 6 as well as the positions 2 and 5 are symmetric and the material properties in these positions are expected to be similar. Variation of mean values of yield and ultimate strength is shown in Figure 3.3. Specimen locations are numbered along the x-axis according to Figure 3.1(b).

Large variation of tensile properties is only observed for the cast iron material IP23T. For other cross-sections the variation of tensile properties is insignificant.

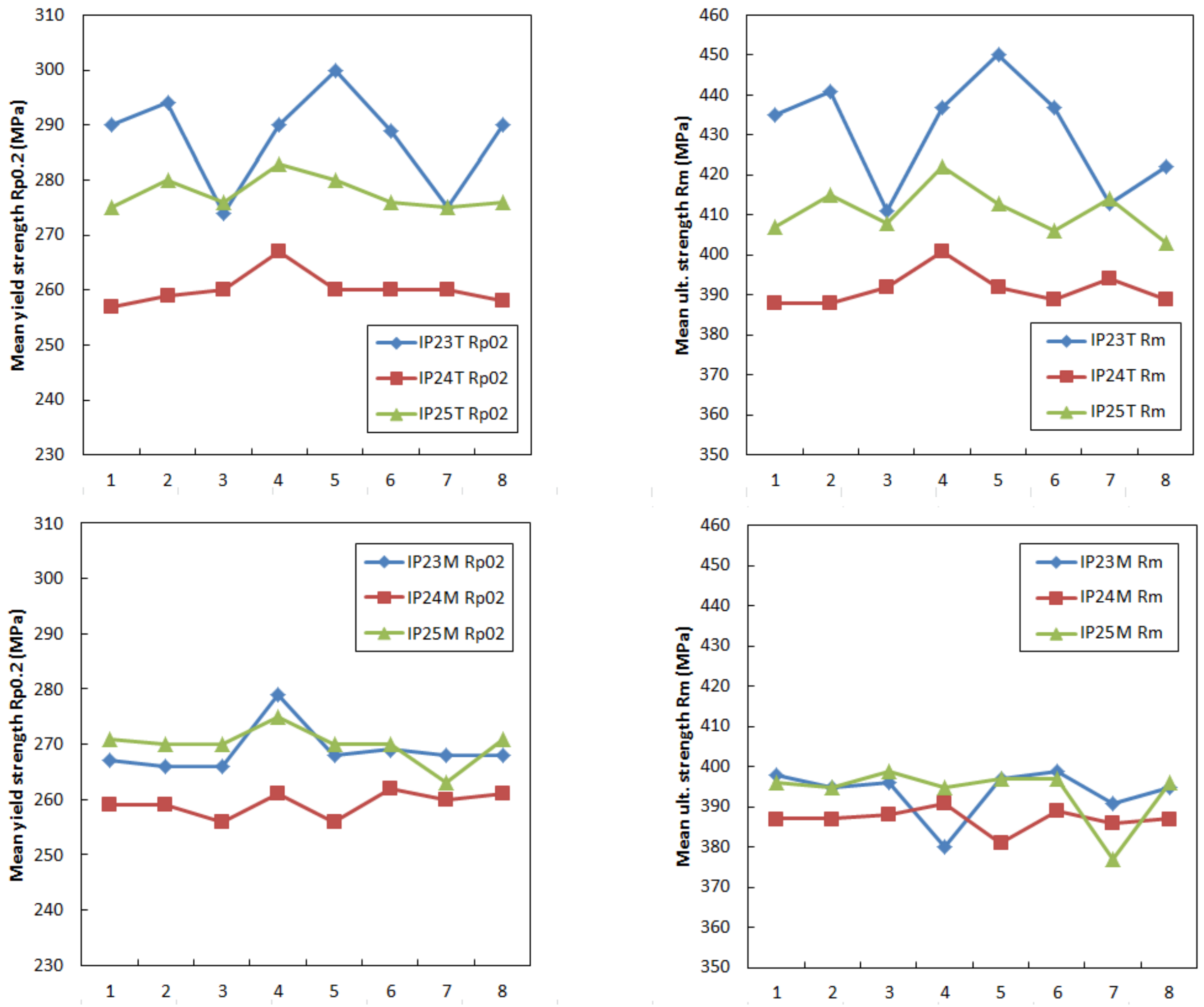

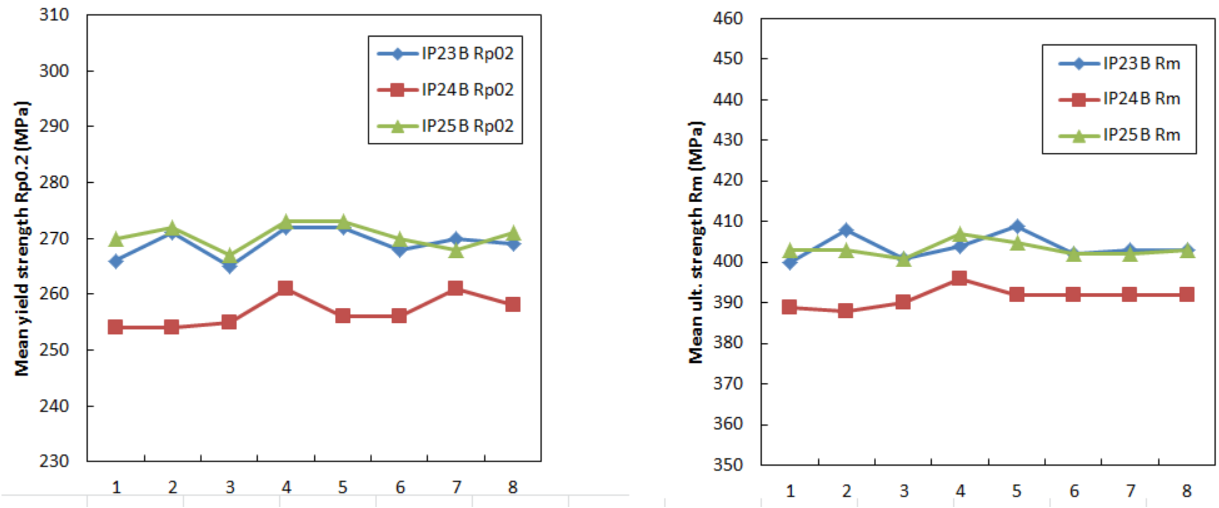

Figure 3.3: Variation of the mean values for yield and ultimate strength plotted as a function of the cross-sectional position. Engineering stress values are presented.

3.1.4 Stress-strain curve in tension

Based on the mean estimate data for tensile properties of the cast iron material, the true stress-strain curve was constructed and shown in Figure 3.4. The tabulated values of true strain and true stress are provided in Table 3.6.

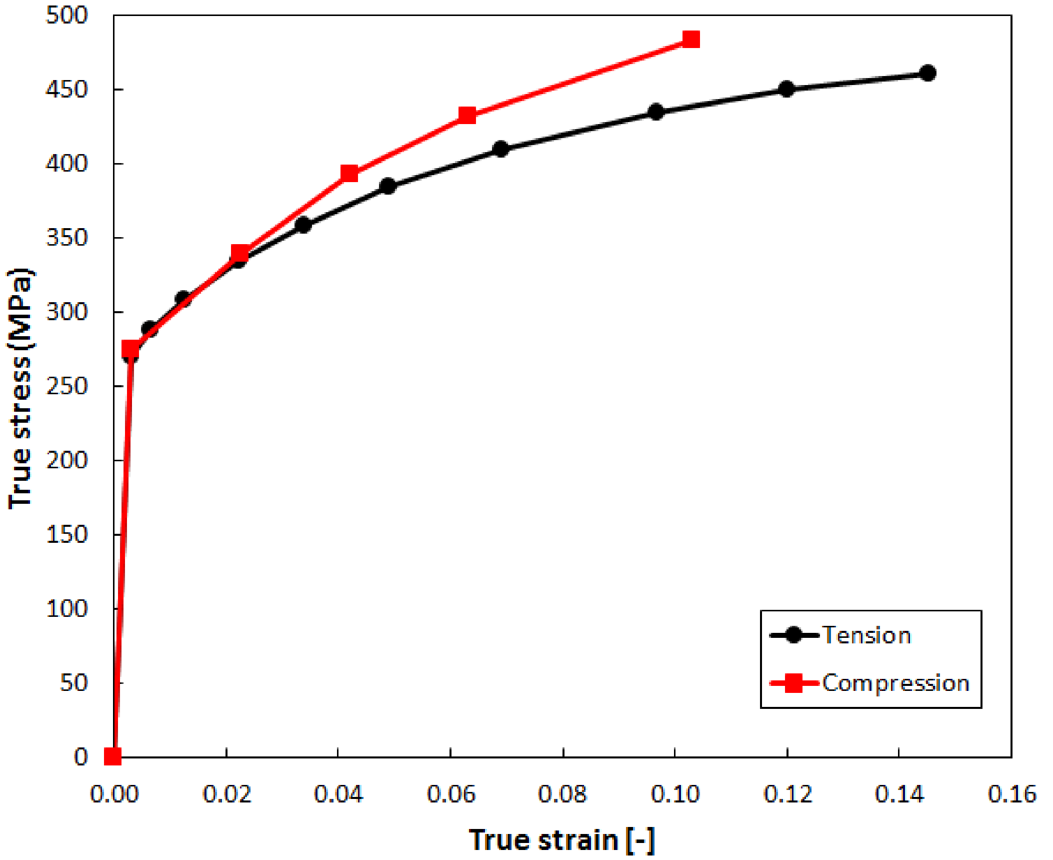

Figure 3.4: Mean trues stress-strain curves in tension and in compression.

Table 3.6: Tabulated data for the true stress-strain curve in tension.

True strain (-)	True stress (MPa)
0.00000	0.0
0.00296	269.8
0.00644	287.7
0.01246	309.0
0.02222	334.1
0.03389	359.0
0.04902	384.1
0.06908	409.1
0.09680	434.0
0.12009	449.5
0.14535	460.5

3.2 Compression tests

3.2.1 Test specimen positions

Compression tests of cast iron material were performed for the PWR-insert IP23M [12] (at the middle position along the vertical axis, see Fig 3.1a). Six specimens have been tested. The location of specimens in the cross-section is unknown.

3.2.2 Test data analysis

Yield strength $R_{p0.2}$ and compression strength at 2%, 4%, 6% and 10% for the cast iron material were measured in compression tests. These properties were statistically evaluated using Eqs. (2.1-2.3) in order to obtain a mean estimate along with the confidence intervals (90% confidence). The results are summarized in Table 3.7.

Table 3.7: Evaluation of all compression test data (engineering stress-strain definition). Compressive strength properties [12] and estimates of the sample mean, standard deviation and population mean (90% confidence).

Specimen	Yield strength $R_{p0.2}$ (MPa)	Strength R_{p2} (MPa)	Strength R_{p4} (MPa)	Strength R_{p6} (MPa)	Strength R_{p10} (MPa)
1	277	352	422	471	-
2	280	355	423	472	552
3	273	351	418	468	546
4	275	350	418	467	542
5	276	353	421	471	549
6	278	355	420	470	546
Sample mean m	276.5	352.7	420.3	469.8	547.0
Sample std. dev. s	2.4	2.1	2.1	1.9	3.7
Population mean μ	$274.5 \leq \mu \leq 278.5$	$350.9 \leq \mu \leq 354.4$	$418.6 \leq \mu \leq 422.0$	$468.2 \leq \mu \leq 471.4$	$543.4 \leq \mu \leq 550.6$

Table 3.8: Evaluation of all compression test data (true stress-strain definition). Compressive strength properties and estimates of the sample mean, standard deviation and population mean (90% confidence).

Specimen	Yield strength at 0.2% strain (MPa)	Yield strength at 2% strain (MPa)	Yield strength at 4% strain (MPa)	Yield strength at 6% strain (MPa)	Yield strength at 10% strain (MPa)
1	276.2	337.5	394.1	434.5	490.3
2	279.3	337.7	395.1	434.6	489.0
3	272.2	333.0	391.3	429.7	480.4
4	274.1	330.9	390.4	427.3	477.7
5	275.2	332.7	391.0	429.9	480.0
6	277	332.9	393.1	431.7	480.3
Sample mean m	275.7	334.1	392.5	431.3	482.9
Sample std. dev. s	2.4	2.8	1.9	2.9	5.3
Population mean μ	$273.7 \le \mu \le 277.7$	$331.8 \le \mu \le 336.4$	$390.9 \le \mu \le 394.1$	$428.9 \le \mu \le 433.7$	$478.6 \le \mu \le 487.3$

3.2.3 Stress-strain curve in compression

Based on the mean estimate data for compression properties of the cast iron material, the true stress-strain curve was constructed and shown in Figure 3.4. The tabulated values of true strain and true stress are provided in Table 3.9.

Table 3.9: Tabulated data for the true stress-strain curve in compression.

True strain (-)	True stress (MPa)
0	0
0.00311	275
0.02248	339.7
0.04210	392.3
0.06303	432.5
0.10303	482.9

3.3 Fracture toughness tests

3.3.1 Test conditions and specimen positions

Fracture toughness tests of cast iron material for PWR-inserts were performed in different environment (air or water at different temperatures). The summary of all fracture toughness testing is presented in Table 3.10. For the PWR-insert IP23T the locations of specimens are marked as shown in Figure 3.5 (a).

Table 3.10: Summary of fracture toughness tests.

Test environment	PWR-inserts (specimens)	Specimen positions	Reference
Air 20 ºC	IP23T (6specimens) IP23M (6 specimens) IP24M (6 specimens) IP25M (6 specimens) IP25M (2 specimens)	1-6 (Fig. 3.5(a)) 1-6 (Fig. 3.5(b)) 1-6 (Fig. 3.5(b)) 1-6 (Fig. 3.5(b)) 7-8 (Fig. 3.5(b))	[13] [14] [15] [16] [17]
Water 20 ºC	IP25M (2 specimens)	7-8 (Fig. 3.5(b))	[17]
Water 10 ºC	IP23M (3 specimens)	N/A	[18]
Water 0 ºC	IP23T (3 specimens) IP23M (3 specimens) IP23B (3 specimens)	N/A	[18]

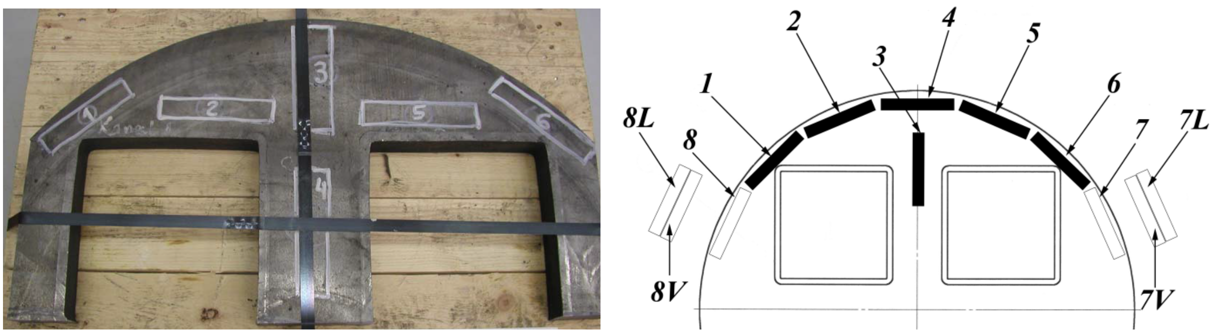

(a) (b)

Figure 3.5: Positions for cutting the specimens for fracture toughness tests (L=Air, V=water).

3.3.2 Test data analysis

Fracture toughness values at initiation and including 2 mm stable crack growth were measured in air environment at 20 ºC and in water environment at 0, 10 and 20 ºC. In some tests, the fracture toughness values could not be qualified as J_{Ic} according to the ASTM E 1820 standard due to uneven and skewed crack front or difference in crack growth increment measured by the compliance method and physically from the fracture surfaces. However, the error in measured mean values of J was assessed to be small. The J-R curves also demonstrate a good quality. Therefore, the J_{crit} values were also used in the evaluation of fracture toughness data.

The fracture toughness data was statistically evaluated using Eqs. (2.1-2.3) in order to obtain a mean estimate along with the confidence intervals (90% confidence). The results are summarized in Tables 3.11-3.18. It can be observed that the fracture toughness data is substantially higher in the air environment than in water.

3.3.2.1 Fracture toughness data in air environment

The results for the fracture toughness data in air environment are summarized below in Tables 3.11-3.15. It can be observed that the mean values of fracture toughness are lower for the specimens from the top (T) position (IP23T specimens in Table 3.11). Other sets of specimens, all taken from the middle (M) position and from all three PWR-inserts (IP23, IP 24 and IP25), demonstrate higher and consistent with each other values of fracture toughness (Tables 3.12-3.14).

Table 3.11: Fracture toughness data for the IP23T (air at 20 ºC) and estimates of the population mean (using α=0.1, i.e. 90% confidence).

Fracture toughness	**Data**	**Sample mean** m	**Sample std. dev.** s	**Population mean** μ
J_{Ic} (kN/m), at initiation	59, 52, 61, 49, 46, 48	52.5	6.2	$47.4 \leq \mu \leq 57.6$
J_{2mm} (kN/m), at 2 mm stable crack growth	140, 126, 136, 111, 102, 127	123.7	14.6	$111.7 \leq \mu \leq 135.7$

Table 3.12: Fracture toughness data for the IP23M (air at 20 ºC) and estimates of the population mean (using α=0.1, i.e. 90% confidence).

Fracture toughness	**Data**	**Sample mean** m	**Sample std. dev.** s	**Population mean** μ
J_{Ic} (kN/m), at initiation	84, 72, 79, 63, 63, 65	71.0	8.9	$63.7 \leq \mu \leq 78.3$
J_{2mm} (kN/m), at 2 mm stable crack growth	164, 148, 166, 155, 150, 141	154.0	9.7	$146.1 \leq \mu \leq 161.9$

Table 3.13: Fracture toughness data for the IP24M (air at 20 ºC) and estimates of the population mean (using α=0.1, i.e. 90% confidence).

Fracture toughness	Data	Sample mean m	Sample std. dev. s	Population mean μ
J_{Ic} (kN/m), at initiation	74, 78, 93, 74, 71, 76	77.7	7.9	$71.2 \le \mu \le 84.1$
$J_{2\mathrm{mm}}$ (kN/m), at 2 mm stable crack growth	169, 159, 184, 167, 156, 175	168.3	10.3	$159.9 \le \mu \le 176.8$

Table 3.14: Fracture toughness data for the IP25M (air at 20 ºC) and estimates of the population mean (using α=0.1, i.e. 90% confidence).

Fracture toughness	Data	Sample mean m	Sample std. dev. s	Population mean μ
J_{Ic} (kN/m), at initiation	57, 65, 69, 67, 58, 79, 75, 64	66.8	7.6	$61.7 \le \mu \le 71.8$
$J_{2\mathrm{mm}}$ (kN/m), at 2 mm stable crack growth	137, 158, 169, 148, 153, 187, 158, 150	157.5	15.1	$147.4 \le \mu \le 167.6$

Table 3.15: All specimens tested in air at 20 ºC. Estimates of the population mean (using α=0.1, i.e. 90% confidence).

Case	Sample mean m	Sample std. dev. s	Population mean μ
J_{Ic} (kN/m)	67.0	11.6	$63.1 \le \mu \le 70.8$
$J_{2\mathrm{mm}}$ (kN/m)	151.4	20.3	$144.6 \le \mu \le 158.2$

3.3.2.2 Fracture toughness data in water environment

The results for the fracture toughness data in water environment are summarized below in Tables 3.16-3.18. Variation of fracture toughness values with the position along a PWR-insert can be studied from Table 3.16 presenting the results for the IP23 insert at the top (T), middle (M) and bottom (B) positions. It can be observed that the fracture toughness values for the IP23M and IP23B specimens are comparable with each other and clearly higher than the values for the IP23T specimens. This observation is consistent with findings from the specimens tested in air environment (see Section 3.3.2.1). It should be underlined though that these findings are based on rather limited number of test data.

Fracture toughness data in water at 20 ºC was only obtained for two specimens from IP25M test set. Fracture toughness values at initiation J_{Ic} were 35 and 39 kN/m, and including 2 mm stable crack growth $J_{2\mathrm{mm}}$ were 108 and 117 kN/m respectively. The IP25M data was not statistically analysed and presented in a separate table. However, the fracture toughness values for water environment at 20 ºC are included in the estimates of the population mean for water environment given in Table 3.18.

In general, a comparison of the facture toughness values obtained in air and water environment can be performed using Table 3.15 and 3.18. The mean values at initiation and at 2 mm stable crack growth are almost twice higher from the tests in air compared with the tests in water.

Table 3.16: Fracture toughness data for the IP23 (water at 0 ºC) and estimates of the population mean (using α=0.1, i.e. 90% confidence).

Case	Fracture toughness	Data	Sample mean m	Sample std. dev. s	Population mean μ
IP23T	J_{Ic} (kN/m)	25, 15, 26	22.0	6.1	$11.7 \leq \mu \leq 32.3$
	J_{2mm} (kN/m)	70, 45, 55	56.7	12.6	$35.5 \leq \mu \leq 77.9$
IP23M	J_{Ic} (kN/m)	29, 41, 35	35.0	6.0	$24.9 \leq \mu \leq 45.1$
	J_{2mm} (kN/m)	96, 94, 93	94.3	1.5	$91.8 \leq \mu \leq 96.9$
IP23B	J_{Ic} (kN/m)	35, 36, 31	34.0	2.6	$29.5 \leq \mu \leq 38.5$
	J_{2mm} (kN/m)	90, 92, 78	86.7	7.6	$73.9 \leq \mu \leq 99.4$

Table 3.17: Fracture toughness data for the IP23M (water at 10 ºC) and estimates of the population mean (using α=0.1, i.e. 90% confidence).

Fracture toughness	Data	Sample mean m	Sample std. dev. s	Population mean μ
J_{Ic} (kN/m), at initiation	38, 38, 33	36.3	2.9	$31.5 \leq \mu \leq 41.2$
J_{2mm} (kN/m), at 2 mm stable crack growth	97, 108, 96	100.3	6.7	$89.1 \leq \mu \leq 111.6$

Table 3.18: All specimens tested in water at 0 ºC, 10 ºC and 20 ºC. Estimates of the population mean (using α=0.1, i.e. 90% confidence).

Case	Sample mean m	Sample std. dev. s	Population mean μ
J_{Ic} (kN/m)	32.6	6.9	$29.3 \leq \mu \leq 35.9$
J_{2mm} (kN/m)	88.5	20.2	$79.0 \leq \mu \leq 98.0$

3.4 Deviation of test results for the IP23T

It is noted from the tensile tests that the yield strength $R_{p0.2}$ and ultimate strength R_m for the top (T) section of IP23 insert are apparently higher than the properties measured in other sections and for other inserts (Fig. 3.2) and demonstrate a significant scatter (Fig. 3.3). The IP23T specimens also demonstrated decreased elongation at failure values and decreased fracture toughness (Table 3.11 and 3.16).

The results of metallographic investigations showed that the top section of the insert IP23 has considerably higher content of pearlite (10-30%) compared to the middle and bottom sections (5-10%). The high amount of pearlite could most certainly affect the material properties in the way described above.

The reason for the high pearlite content in the top section is due to abnormal process deviation. During casting a substantial amount of molten metal disappeared due to leak in the mould. The remaining volume of molten metal was adequate to produce the complete insert IP23 but insufficient to create the extra length (feeder) that is normally required. The purpose of a feeder is to collect slag and other impurities. It is also required to achieve a proper solidification and cooling rates. The absence of the feeder during casting of the IP23 insert resulted in increased pearlite content in the top section of the insert.

In order to investigate to what extent the statistical estimates of mean values, standard deviation and confidence intervals are affected by the data from the IP23T, the statistical analyses were repeated excluding the IP23T values. The results are presented below.

3.4.1 Tensile properties

The statistical analysis results of all tensile data excluding the IP23T values are given in Tables 3.19-3.21. These tables correspond to the equivalent Tables 3.4-3.6. A comparison of the results shows that the mean values for the yield and ultimate strength are decreased. The scatter is also reduced.

Table 3.19: Evaluation of all tensile data (engineering stress-strain definition). Tensile properties and estimates of the population mean (90% confidence).

All tensile data (without IP23T)	**Yield strength** $R_{p0.2}$ **(MPa)**	**Ultimate strength** R_m **(MPa)**	**Elongation at failure** A **(%)**
Sample mean m	267.0	397.1	16.9
Sample standard deviation s	6.8	8.5	4.2
Population mean μ	$265.7 \leq \mu \leq 268.3$	$395.5 \leq \mu \leq 398.8$	$16.1 \leq \mu \leq 17.7$

Table 3.20: Evaluation of all tensile data (true stress-strain definition). Tensile properties and estimates of the population mean (90% confidence).

All tensile data (without IP23T)	**Yield strength (MPa)**	**Ultimate strength (MPa)**	**Elongation at failure (%)**
Sample mean m	267.8	457.9	14.8
Sample standard deviation s	6.9	17.4	3.2
Population mean μ	$266.5 \leq \mu \leq 269.1$	$454.6 \leq \mu \leq 461.3$	$14.2 \leq \mu \leq 15.4$

Table 3.21: Tabulated data for the true stress-strain curve in tension.

True strain (-)	**True stress (MPa)**
0.00000	0.0
0.00302	267.8
0.00657	284.7
0.01270	306.4
0.02266	331.5
0.03457	356.4
0.05000	381.5
0.07046	406.5
0.09873	431.4
0.12249	446.9
0.14826	457.9

3.4.2 Fracture toughness properties

The statistical analysis results of all fracture toughness data excluding the IP23T values are given in Tables 3.22 and 3.23. These tables correspond to the equivalent Tables 3.15 and 3.18. A comparison of the results shows that the mean values for the fracture toughness are increased. The standard deviation is substantially reduced.

Table 3.22: All specimens tested in air at 20 ºC (**without IP23T**). Estimates of the population mean (using α=0.1, i.e. 90% confidence).

Case	Sample mean m	Sample std. dev. s	Population mean μ
J_{Ic} (kN/m)	71.3	9.0	$67.8 \leq \mu \leq 74.8$
J_{2mm} (kN/m)	159.7	13.1	$154.6 \leq \mu \leq 164.8$

Table 3.23: All specimens tested in water at 0 ºC, 10 ºC and 20 ºC (**without IP23T**). Estimates of the population mean (using α=0.1, i.e. 90% confidence).

Case	Sample mean m	Sample std. dev. s	Population mean μ
J_{Ic} (kN/m)	35.5	3.5	$33.5 \leq \mu \leq 37.4$
J_{2mm} (kN/m)	97.2	10.5	$91.4 \leq \mu \leq 102.9$

Because of the process deviation for insert IP23, it is recommended to use fracture toughness data without IP23T when performing a damage tolerance analysis.

4 COMPARISON WITH OTHER DATA FOR BWR- AND PWR-INSERTS

4.1 Comparison with other data for PWR-inserts

Inspecta has performed a damage tolerance analysis of the PWR iron insert both in the case of a glacial pressure load and in the case of an earthquake induced rock shear load [20]. This analysis was performed using data from inserts IP17 and IP19. When comparing the data from this analysis [20] and the data presented in this report the following conclusions can be made:

- Regarding the stress-strain curve in tension, that is used when doing a damage tolerance analysis in the case of an earthquake induced rock shear load, there is almost no difference between the two curves.
  - The difference in yield strength, at 0.2% strain, is ~1.4%.
  - The difference in yield strength, at ~10% strain, is ~2.1%.
- Regarding the stress-strain curve in compression, that is used when doing a damage tolerance analysis in the case of a glacial pressure load, there is almost no difference between the two curves.
  - The difference in yield strength, at 0.2% strain, is ~0.5%.
  - The difference in yield strength, at 10% strain, is ~1.4%.
- Regarding the fracture toughness data, which is used when doing a damage tolerance analysis, both in the case of a glacial pressure load and in the case of an earthquake induced rock shear load, there is a large difference in the fracture toughness data.
  - The fracture toughness data for PWR-inserts in this report is much better than for PWR-inserts in [20], the reason for this is that PWR-inserts in [20] are tested in water (at 0°C) and PWR-inserts in this repost are tested in air (at 20°C). This difference is mainly related to the testing conditions (water or air) and not the testing temperature. This has been shown in a study conducted in both water and air (at 20°C) [17].

4.2 Comparison with data for BWR-inserts

Inspecta has performed different damage tolerance analysis of the BWR iron insert both in the case of a glacial pressure load [21] and in the case of an earthquake induced rock shear load [22, 23]. When comparing the data from these analyzes [21-23] and the data presented in this report the following conclusions can be made:

- Regarding the stress-strain curve in tension, that is used when doing a damage tolerance analysis in the case of an earthquake induced rock shear load, there is only a small difference between the two curves (except for the standard deviation, which is related to variation at the top position in this report).
  - Yield strength, mean value (BWR) = 280 MPa.
  - Yield strength, standard deviation (BWR) = 6.8 MPa.
  - Yield strength, mean value (PWR) = 270 MPa.
  - Yield strength, standard deviation (PWR) = 9.9 MPa.
  - Ultimate strength, mean value (BWR) = 449 MPa.
  - Ultimate strength, standard deviation (BWR) = 6.4 MPa.
  - Ultimate strength, mean value (PWR) = 462 MPa.
  - Ultimate strength, standard deviation (PWR) = 18.3 MPa.
  - Elongation at failure, mean value (BWR) = 14.8%.
  - Elongation at failure, standard deviation (BWR) = 1.6%.
  - Elongation at failure, mean value (PWR) = 14.8%.
  - Elongation at failure, standard deviation (PWR) = 3.3%.

- Regarding the stress-strain curve in compression, that is used when doing a damage tolerance analysis in the case of a glacial pressure load, there is almost no difference between the two curves.
  - The difference in yield strength, at 0.2% strain, is ~2.1%.
  - The difference in yield strength, at 10% strain, is ~0.2%.
- Regarding the fracture toughness data, which is used when doing a damage tolerance analysis, both in the case of a glacial pressure load and in the case of an earthquake induced rock shear load, there is a large difference in the fracture toughness data.
  - The fracture toughness data for PWR-inserts in this report is much better than for BWR-inserts in [22], the reason for this is that BWR-inserts are tested in water (at 0°C) and PWR-inserts are tested in air (at 20°C). This difference is mainly related to the testing conditions (water or air) and not the testing temperature. This has been shown in a study conducted in both water and air (at 20°C) [17].

5 CONCLUSIONS

SKB has commissioned Inspecta Technology AB to perform a statistical data analysis of material properties for cast iron PWR-inserts IP23, IP24 and IP25. The test data from tension, compression and fracture toughness tests were analysed.

The main purpose of the performed statistical analysis was to obtain the estimates of material properties with a given confidence (90% confidence was used in the analyses). Approximate confidence intervals using the so-called Student's *t*-distribution and the χ^2-distribution were calculated for all measured properties of the cast iron material. These confidence intervals provide a range where the true value of a material property is expected to lie.

Additionally, the performed analysis was aimed to investigate; 1) the variation of material properties between different PWR-inserts and 2) the variation of properties depending on the position where the specimens were taken.

The short conclusions of this investigation are following;

- Variation of properties between different PWR-inserts could be best studied from the tensile test results as substantial amount of data was collected. It could be observed that the yield strength and ultimate strength were lower for the material from the PWR-insert IP24. The tensile properties from the IP23 and IP25 inserts were higher and comparable with each other.

- Certain variation of tensile properties along the insert height was observed from the test data. For all tested PWR-inserts the mean values of the yield strength and the ultimate strength at the top (T) position were higher than for the middle and the bottom positions.

- Large variation of tensile properties depending on the cross-sectional position of a specimen was only observed for the cast iron material IP23T. For other PWR-inserts and tested cross-sections the variation of tensile properties was insignificant.

- Compression properties were only measured for the IP23M material. The variation of the properties depending on the cross-sectional position of the specimens was insignificant.

- Fracture toughness values appear to be somewhat lower for the specimens from the top (T) position in comparison with the middle and the bottom positions. The mean values of fracture toughness at initiation and at 2 mm stable crack growth were almost twice higher from the tests in air compared with the tests in water.

- Because of the process deviation for insert IP23, it is recommended to use fracture toughness data without IP23T when performing a damage tolerance analysis.

6 REFERENCES

[1] AYYUB, B. M., and R. H. MCCUEN., (1997), *Probability, Statistics & Reliability for Engineers*, CRC Press LLC, Boca Raton, Florida.

[2] LISELL, R., (2013-10-24), ”Materialprovning av segjärnsinsats IP23HB”, Undersökningsrapport Nr 1814-1, Swerea SweCast AB, SKBdoc 1369691, version 2.0, Svensk Kärnbränslehantering AB.

[3] LISELL, R., (2013-10-24), ”Materialprovning av segjärnsinsats IP23B”, Undersökningsrapport Nr 1456-1, Swerea SweCast AB, SKBdoc 1348282, version2.0, Svensk Kärnbränslehantering AB.

[4] LISELL, R., (2013-10-24), ”Materialprovning av segjärnsinsats IP23M”, Undersökningsrapport Nr 1455-1, Swerea SweCast AB, SKBdoc 1348281, version 2.0, Svensk Kärnbränslehantering AB.

[5] LISELL, R., (2013-10-24), ”Materialprovning av segjärnsinsats IP23T”, Undersökningsrapport Nr 1424-1, Swerea SweCast AB, SKBdoc 1348258, version 2.0, Svensk Kärnbränslehantering AB.

[6] LISELL, R., (2013-10-24), ”Materialprovning av segjärnsinsats IP24B”, Undersökningsrapport Nr 1870-1, Swerea SweCast AB, SKBdoc 1372047, version 2.0, Svensk Kärnbränslehantering AB.

[7] LISELL, R., (2013-10-24), ”Materialprovning av segjärnsinsats IP24M”, Undersökningsrapport Nr 1869-1, Swerea SweCast AB, SKBdoc 1371794, version 2.0, Svensk Kärnbränslehantering AB.

[8] LISELL, R., (2013-10-24), ”Materialprovning av segjärnsinsats IP24T”, Undersökningsrapport Nr 1724-1, Swerea SweCast AB, SKBdoc 1364251, version 2.0, Svensk Kärnbränslehantering AB.

[9] LISELL, R., (2013-10-24), ”Materialprovning av segjärnsinsats IP25B”, Undersökningsrapport Nr 2105-1b, Swerea SweCast AB, SKBdoc 1388648, version 2.0, Svensk Kärnbränslehantering AB.

[10] LISELL, R., (2013-10-24), ”Materialprovning av segjärnsinsats IP25M”, Undersökningsrapport Nr 2104-1b, Swerea SweCast AB, SKBdoc 1387918, version 2.0, Svensk Kärnbränslehantering AB.

[11] WIHED, M., (2013-10-24), ”Materialprovning av segjärnsinsats IP25M-2270”, Undersökningsrapport Nr 2329-1, Swerea SweCast AB, SKBdoc 1398936, version 2.0, Svensk Kärnbränslehantering AB.

[12] PERSSON, H., (2013-02-05), “Stukprovning på gjutjärnsinsats IP23M”, Provningsrapport PRO13-0157, Utg. 1, Exova AB, SKBdoc 1378752, version1.0, Svensk Kärnbränslehantering AB.

[13] ÖBERG, M., (2013-08-08), ”Brottmekanisk provning av segjärn, IP23T”, Rapport SKB130808, KTH Hållfasthetslära, SKBdoc 1403709 version2.0, Svensk Kärnbränslehantering AB.

[14] ÖBERG, M., (2013-05-23), ”Brottmekanisk provning av segjärn, IP23M”, Rapport SKB130518-2, KTH Hållfasthetslära, SKBdoc 1397325, version 3.0, Svensk Kärnbränslehantering AB.

[15] ÖBERG, M., (2013-05-23), ”Brottmekanisk provning av segjärn, IP24M”, Rapport SKB130518-3, KTH Hållfasthetslära, SKBdoc 1397324, version 3.0, Svensk Kärnbränslehantering AB.

[16] ÖBERG, M., (2013-05-23), ”Brottmekanisk provning av segjärn, IP25M”, Rapport SKB130518-4, KTH Hållfasthetslära, SKBdoc 1397930, version 3.0, Svensk Kärnbränslehantering AB.

[17] ÖBERG, M., (2013-05-18), ”Brottmekanisk provning av segjärn, IP25M”, Rapport SKB130518, KTH Hållfasthetslära, SKBdoc 1397931, version 3.0, Svensk Kärnbränslehantering AB.

[18] ÖBERG, M., (2013-10-18), ”Brottmekanisk provning av gjutjärn, IP23T, IP23B och IP23M”, Rapport SKB121108, KTH Hållfasthetslära, SKBdoc 1369688, version 4.0, Svensk Kärnbränslehantering AB.

[19] LISELL, R., (2013-10-24), ”Materialprovning av segjärnsinsats IP25T”, Undersökningsrapport Nr 1988-1c, Swerea SweCast AB, SKBdoc 1375086, version 2.0, Svensk Kärnbränslehantering AB.

[20] DILLSTRÖM, P., BOLINDER, T., and E. BONNAUD., (2013-10-01), “Analysis of PWR canister inserts using data acquired from PWR material”, Technical Report 50010510-1, Rev. 3, Inspecta Technology AB, SKBdoc 1288288 - version 2.0.

[21] DILLSTRÖM, P., ALVELIND, L. and ANDERSSON, M., (2010-01), “Framtagning av acceptanskriterier samt skadetålighetsanalyser för segjärnsinsatsen”, SKB Rapport R-10-11, Svensk Kärnbränslehantering AB.

[22] DILLSTRÖM, P. and BOLINDER, T., (2010-10), “Damage tolerance analysis of canister inserts for spent nuclear fuel in the case of an earthquake induced rock shear load”, SKB Technical Report TR-10-29, Swedish Nuclear Fuel and Waste Management Co.

[23] DILLSTRÖM, P., and ALVERLIND, L., (2013-12), “Probabilistic analysis of BWR canister inserts for spent nuclear fuel in the case of an earthquake induced rock shear load”, Technical Report 50014130-1, Rev. 0, Inspecta Technology AB, SKBdoc 1412158 - version 1.0.

7 TABLE OF REVISIONS

Rev.	Activity / Purpose of this revision	Handled by	Date
0	—	Andrey Shipsha	2013-11-13
1	All sections: Editorial comments. Section 3.1.2: Text discussing the results in Table 3.4 and Table 3.5 is added. Section 3.1.4: Figure 3.4 is updated to include the true stress-strain curve in compression. Section 3.2.3: Figure 3.5 is removed as the curve was added to Fig. 3.4. Section 3.3.1. Figure 3.6 is re-numbered to Fig. 3.5. Figure 3.5(b) is new. Section 3.3.2: Text discussing fracture toughness testing is added. Section 3.4: New section, excluding test results for IP23T. Section 4: New section to compare with other data sets. Section 6: Missing reference [19] is added. All references are updated with SKBdoc reference.	Andrey Shipsha	2013-12-03
2	The missing curves from the tensile tests of IP25M set (8 specimens) and for the specimen #2 from the IP25B set have been obtained and analysed. Small changes are introduced in Tables 3.5, 3.6, 3.20 and 3.21. The Figure 3.4 is updated. The report has been updated with regard to the SKB review comments (SKB 1419243).	Andrey Shipsha	2013-12-22